Effects of monovalent and divalent ions in coal gasification brine on the froth entrainment and flotation kinetics of anthracite coal

Kaidi Zheng [1], **Xiangning Bu** [1], **Shaoqi Zhou** [1], **Jing Zhang** [2], **Huaizhi Shao** [3], **Jie Sha** [1], **Guangyuan Xie** [1]

[1] Key Laboratory of Coal Processing and Efficient Utilization (Ministry of Education), School of Chemical Engineering and Technology, China University of Mining and Technology, Xuzhou 221116, China

[2] Department of Computer Science, Emory University, Atlanta, Georgia, 30324 USA

[3] School of Resources and Environmental Engineering, Shandong University of Technology, Zibo 255049, China

Corresponding authors: shajie@cumt.edu.cn, xiangning.bu@cumt.edu.cn, shaohuaizhicumt@outlook.com

Abstract: Water plays a critical role in various stages of flotation, which brings a lot of pressure to the flotation processing plants resided in dry areas. In this regard, it will be of significance to explore the feasibility of using wastewater resources in mineral flotation. Coal gasification brine (*CGB*) that contains a high concentration of salts becomes the subject of interest of this study. In this study, a synthetic *CGB* solution, which was prepared by adding NaCl, $MgCl_2$, and $CaCl_2$ to ultrapure water based on the composition of salts in a real *CGB*, was used in the flotation of anthracite coal. The comparison results based on the first-order model showed that flotation in the presence of the synthetic *CGB* solution gave a higher flotation selectivity (*SI* =7.086) than that of flotation in ultrapure water (*SI*=3.545). Water recoveries and average bubble sizes in the froth showed that the addition of the three salt ions (Na^+, Mg^{2+}, and $Ca2^+$) was conducive to diminishing the entrainment of gangue materials as a result of the reduction of water reporting to the froth. Additionally, the zeta potentials and induction time measurements indicated that only divalent ions of Ca^{2+} and Mg^{2+} significantly compressed the double electrical layer and enhanced the attachment between bubbles and coal particles according to DLVO theory, which was further confirmed by the calculation of interaction energy between coal and bubbles. The findings of the present work may promote the use of *CGB* as a potential water resource in coal flotation.

Keywords: coal gasification brine, salt ions, coal flotation, entrainment, flotation kinetics, DLVO theory

1. Introduction

The daily operation of a coal preparation plant highly relies on the use of a large amount of water, which is a non-renewable nature resource (Gupta et al., 2012). As such, coal preparation plants are required to realize a closed cycle of washing water that can not only reduce sewage discharge but also relieve pressure on the usage of fresh water (Bournival et al., 2017). However, the implementation of closed water circuits has caused the processing water to be gradually enriched of various inorganic ions that come from different sources, including the chemical additives, the groundwater, or sea water with high salinity (Wang et al., 2014). Bournival et al. (2019) continuously monitored the conductivity of the processing water taken from the tailing streams in a flotation plant for over two years, and the results showed that the conductivity value of the processing water greatly increased to 16 ms/cm from 7 ms/cm.

Many studies have shown that inorganic electrolytes presented in water affect the contact angle of coal particles. Klassen and Mokrousov (1963) found that the contact angle of coal particles in NaCl solutions increased with the increasing salt concentration. However, there is extensive debate in the literature regarding the contact angle of coal particles in presence of electrolytes. Laskowski and Iskra

(1970) found that contact angles measured on two methylated silica plates did not change with the increasing KCl concentration. Ozdemir et al. (2009) found that the contact angle value of a flat coal surface in bore water was the same with that in pure water. Similar conclusions have been made by Yoon and Sabey (1983) according to the measurements of contact angle angles of coal particles in the presence of sodium salts or sulphate salts. It is hypothesized that instability and thinning of the hydrated layer at the surface of the coal particle occurs when ions are present, which increases the particle surface hydrophobicity (Yang et al., 1988). Meanwhile, the addition of electrolytes compressed the electrical double layer (Fuerstenau et al., 1983) The lower double layer thickness is conducive to the reduction in the electrostatic interactions between particles and bubbles, and between particles and particles due to the double layer thickness, resulting in an increase in the bubble-particle collision probability (Xu and Yoon, 1990; Li and Somasundaran, 1993; Pugh et al., 1997).

The fundamental steps of the interaction between particles and bubbles are contact of the particles with the bubbles, followed by film rupture and attachment (Ye and Miller, 2007). The times during which these phenomena occur are usually called the contact time and induction time, respectively. The physics of the system is the determining factor for the contact time, while the hydrophobic features of the particle surface is the physicochemically dominated factor for the induction time. The measurement results of the induction time are widely used to compare the bubble-particle interaction (Bu et al., 2019; Ye and Miller, 1988; Yoon and Yordan, 1991).

Many researchers have also observed that flotation performance coal particles are greater in salt solution than in distilled water. Flotation of coal is lower in distilled water than in tap water or ion augmented water (Arnold and Aplan, 1986). At low salt concentrations (below $0.1 \ mol/dm^3$), the flotation recovery of coal particles decreases with an increase in salt exhibiting a minimum at around pH 6 and a maximum between pH 7 and 9. With the further increase of salt concentration, however, flotation recovery exhibiting a marked increase in flotation with salt concentration (Li and Somasundaran, 1993). Yoon (1982) found that the flotation responses in terms of separation efficiency (defined as combustible recovery-ash recovery) were comparable to those achieved with conventional flotation. When the flotation rate constants were compared, the kinetics of the flotation in the presence of salts was faster than that of conventional flotation (Yoon, 1982). Harvey et al. (2002) showed that in low electrolyte concentration solutions coal flotation decreased with the increase in salt concentration, but in high electrolyte concentration solutions, coal flotation was increased with the salt concentration. According to the differences in the flotation recovery in different salt solutions, Pugh et al. (1997) classified those electrolytes into three distinct groups. Group A electrolytes of divalent and trivalent cations were found to give the best flotation response compared to electrolytes of group B (NaCl, LiCl, KCl, CsCl, NH_4Cl), and group C (NaAc, $NaClO_4$, $HClO_4$, HCl, H_2SO_4, $LiClO_4$). Kurniawan et al. (2011) found that in the presence of Dowfroth 250, $MgCl_2$ gave the most stable froth, while $NaClO_3$ showed the lowest froth stability that was similar to the recovery response (Kurniawan et al.,2011; Ozdemir 2013). Wang et al. (2014) conducted a review addressing the effect of saline water on the interfacial phenomena taking place in the flotation process, such as surface wettability, bubble-particle collision and attachment, mineral particle interactions and frothing. Ersoy et al. (2013) and Ozdemir et al. (2018) suggest that under the present test conditions, it is possible to float thermally treated lignite samples of partially hydrophobic character in salt solutions in the absence of collector and frother. The work conducted by Wei et al. (2016) investigated the effect of processing water containing sodium, potassium, calcium, and magnesium ions with other anions to flotation, and the results showed that the froth stability increased due to the addition of the metal ions. The results also showed that there existed an interaction effect between MIBC (Methyl Isobutyl Carbinol) and the salt ions, which would diminish the flotation combustible matter recovery. While Li et al. (2017) explained this may be attributed to the increase in the pulp viscosity based on their study regarding the effect of sodium chloride in saline water on coal flotation. Moreover, it has been reported that the flotation recovery of oxidized coals was more effective in the presence of salt ions under acidic conditions, and the maximum combustible matter recovery was achieved at pH 6 (Wang et al., 2019).

Coal gasification brine (*CGB*) which is generated in the reuse of coal gasification wastewater, contains high concentrations of salt ions ($35,000 \ mg/dm^3$ the total dissolved solids) and several organic compounds ($1000 \ mg/dm^3$ the chemical oxygen demand) (Fang and Han, 2018). With the increasing

awareness of environmental issues and tight environmental regulations, zero liquid discharge is strictly required to improve water utilization efficiency and protect the environment (Jia et al., 2015). Currently, the deficiencies of serious membrane fouling and the production of huge quantities of unusable salt-mixtures constrains the application of the conventional technology for treating *CGB* integrating the processes of reverse osmosis, evaporation, and crystallization (Jia et al., 2016). Large attention has been paid to economic and efficient technologies that exhibit both excellent rejections of multivalent ions and organic compounds. Considering that zero liquid discharge and the reuse of brine from coal gasification wastewater remarkably reduces the expenditure of salts, the brine should be regarded as a resource rather than a waste (Li et al., 2018). *CGB* has similar properties of saline water and industrial wastewater from a perspective of salt ions, which is highly possible to be employed as a processing water resource for coal flotation.

The literature, as stated above, indicates that different ions have different effects on the recovery of combustible content. However, the prior research regarding to the effects of salt ions on coal flotation was only concentrated on the use of saline water and industrial wastewater (Wang and Peng, 2014; Wang et al., 2019; Gamal et al., 2018). What's more, there are few studies on the flotation performance of coal in the presence of *CGB*. Moreover, the influencing degree of various cations (Na^+, Mg^{2+}, Ca^{2+}) in CGB on bubble-particle induction time, froth entrainment, and flotation kinetics have been studied rarely.

In this purpose, this study was aimed to investigate the effect of simulated *CGB* solutions consisting of a single salt ion (Na^+, Mg^{2+}, and Ca^{2+}) and three mixed salt ions on to the flotation recovery of fine coal particles were explored by conducting a series of flotation experiments. The results were evaluated using the selectivity index and flotation rate constant (according to the classical first-order model) in conjunction with the measurements of induction time and zeta potential. Different evaluation indicators, e.g. induction time, froth entrainment and floatation kinetics were measured or calculated to investigate the influencing degree of three common salt ions in *CGB*, which could be instructive and meaningful for developing the coal flotation process in the water-deficient mining area.

2. Experimental

2.1. Materials

In this study, analytical grade $CaCl_2$, $NaCl$, $MgCl_2$ (Xilong, China) were used as electrolytes. MIBC [99% of $(CH_3)_2CHCH_2CH(OH)CH_3$] (Aladinin, China) was used as a frother. Kerosene (a mixture of hydrocarbons) was collected from a local gas station. All experiments were conducted with ultrapure water.

The coal sample used in this study was a flotation feed procured from Zhaozhuang coal plant, Shanxi Province, China. Table 1 presents the results of the proximate analysis of the coal sample. The ash content of the coal was 37.21% as seen from table 1, it needs to be reduced in order to meet the standard of utilization. The < 0.5 mm fraction in the as-received sample was screened out and used in the following flotation experiments. As shown in Table 2, the size of coal particles was larger than 0.074 mm accounts for about 55% of the sample, and the ash content of each size fraction increases from 30.11% to 45.22% as the particle size decreases. The simulated *CGB* solution was prepared according to the previous study (Li et al., 2018; Xiong et al., 2015) by dissolving Na^+, Mg^{2+}, and Ca^{2+} salts in ultrapure water. The ultrapure water in these experiments was supplied by Heal Force Super Series Easy Ultra-pure Water System which produced in Shanghai Kanglei Analytical Instrument Co., Ltd. The resistivity of the ultrapure water is greater than 10.0 MΩ. cm. The composition of *CGB* used for the experiments is shown in Table 3. The concentration of Na^+ is the highest while the salt concentrations between Mg^{2+} and Ca^{2+} have no significant difference.

Table 1. Proximate analysis of the coal sample

M_{ad} (%)	A_{ad} (%)	V_{ad} (%)	FC_{ad} (%)
1.44	37.21	24.11	37.24

M_{ad}: moisture of air-dried basis, A_{ad}: ash content on air dried basis, V_{ad}: volatile matter content on air dried basis

FC_{ad}: fixed carbon content on air dried basis

Table 2. Size and ash content distribution of the coal sample

Size fraction (mm)	Yield (%)	Ash Content (%)
0.500-0.250	11.73	30.11
0.250-0.125	22.69	32.10
0.125-0.074	20.08	32.94
0.074-0.045	11.86	33.86
<0.045	33.64	45.22
Total	100.00	

Table 3. The ions composition of *CGB*

Ions	Na^+	Mg^{2+}	Ca^{2+}	Cl^-
Concentration (mg/dm³)	19900	497	461	---

2.2. Methods

2.2.1. Flotation experiments

Flotation experiments were conducted in a sub-aeration flotation cell (RK/FD-II) under a given operating condition: 1900 rpm impeller speed, 2.5 dm³/min air flow rate, and 3 min flotation time. In a given test, 30 g coal sample was added into a specific type of flotation solution for 2 min conditioning. After that, 24 mg kerosene and 7.5 mg MIBC were added into the slurry and the conditioning time for each reagent was kept as 2 min. After the introduction of air, four concentrates were collected at the cumulative times of 0.5, 1, 2, and 3 min after the flotation began. During the flotation, the height of the froth layer was kept at 1 cm by adding the corresponding flotation solution to maintain a constant pulp volume. The flotation solution included ultrapure water, a saline solution consisting of a single salt, and a saline solution consisting of three different salts.

The recovery of combustible matter, the recovery of ash materials, and average water recovery of the four samples were calculated using Eqs. 1, 2, and 3:

  • Recovery of combustible matter:

$$(\%)=\frac{\gamma_C(100-A_C)}{(100-A_F)}\times100 \tag{1}$$

  • Recovery of ash materials:

$$(\%)=\frac{\gamma_C A_C}{A_F}\times100 \tag{2}$$

where the subscript c refers to the concentrate, the subscript F represents the feed, γ_C is the yield of the concentrate, and A is the ash content. The calculation equation of combustible content recovery is in line with ash recovery.

Eq. (3) was used to calculate the water recovery in the concentrates:

$$\text{Average water recovery}=\frac{W_C}{T} \tag{3}$$

where W_C is the weight of water covered in various flotation time, and T is the time that was used for collecting the water in the flotation test.

Froth videos were obtained by a camera rest on a tripod beside the flotation machine. The experimental set-up is presented in Fig 1. The camera was in working condition during the flotation to record the froth formed at the beginning of bubbles' appearance.

2.2.2 Induction time measurement

In this study, the coal particles with sizes ranging from 0.125 to 0.25 mm were used for the induction time measurement by a 2015EZ induction timer (University of Alberta, Canada). The induction time was a valid parameter to evaluate the time required to form an attachment between a particle and a

bubble (Yoon and Yordan, 1991；Verrelli and Albijanic, 2015). The measurement procedure has been described in the literature (Bu et al., 2019). In a given test, a certain amount of 1g coal sample was premixed with a volume of 30 mm saline solution of a known amount of salt ion. After that, the suspension was transported to the transparent sample cell of the Induction timer. Before conducting the measurement, the coal particles in the suspension were allowed to settle until forming a flatbed at the bottom of the cell. During the measurement, the bubble approaching speed was kept at 2.23 cm/s and the capillary bubbles sizes were controlled about 1.3 mm. At each condition, ten observations were repeated for different positions of the flatbed. The results of the attachment were given by a charge-coupled device (CCD) camera. In order to establish the distribution of the induction time (τ), the contact time was then changed by adjusting the pulse frequency. The τ values were recorded when the time at which five out of ten observations resulted in air bubble-particle attachment (Ye and Miller, 1988).
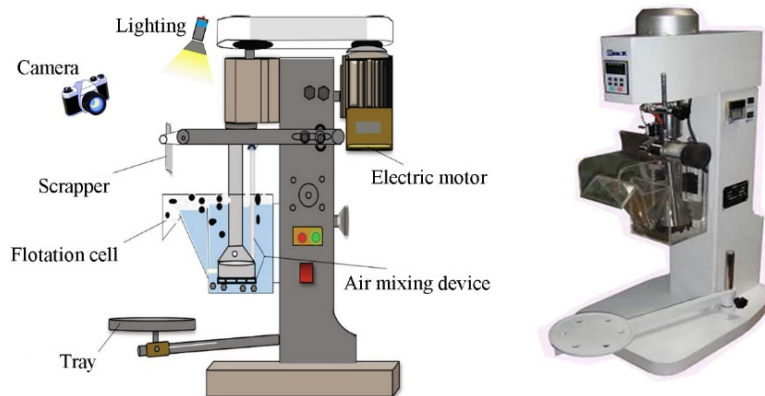
Fig. 1. Experimental set-up for the flotation experiments (left: schematic diagram, right: physical photo). Adapted from the literature (Zhou et al., 2020; Bu et al., 2018)

2.3. Zeta potential measurement of particles

The zeta potential measurements of the coal sample were carried out by the Zeta Plus (Brookhaven, US). The coal sample (< 0.045 mm) used in these measurements was obtained by grinding the < 0.5 mm coal sample in a ball mill for 4 h. Then, 0.1 g coal samples were dispersed in 100 cm^3 single saline solutions and ultrapure water (solids ratio was 0.1%). The concentration was the same as the solution used in flotation. After sedimentation for 24 h, the supernatant liquid in the transparent cells was used to measure the zeta potential with Zeta Plus. Each test was repeated three times and the experimental error was estimated using standard deviation error bar.

2.4. Zeta potential measurement of bubbles

Nano-bubbles were made to measure the zeta potentials with Zeta Plus (Brookhaven, US). Single saline solutions and ultrapure water were treated in the hydrodynamic cavitation (HC) system to get stable bubbles. Two peristaltic pumps (TL00-700M), venturi tube, and 82# tube compose the HC system together with a pulp barrel, and the narrowest part is 3 mm long in the venturi, as shown in Fig 2. Detailed operating procedures for the HC system can be found in the literature (Zhou et al., 2020). The throat velocity of the venturi tube was 16.50 m/s. The 500 cm^3 single saline solution and ultrapure water were treated five loops separately with the HC system. At last, keep the treated solution in test tubes for 12 h and collect 1 cm^3 to measure the zeta potentials of nano-bubbles.

2.5. Calculation of selectivity index

Many kinetic models have been proposed to analyze flotation time-recovery profiles by different investigators (Bu et al., 2017c). The most popular flotation model is the classical first-order flotation model (Bu et al., 2017a):

$$R(t) = R_{\infty}[1 - \exp(-kt)] \tag{4}$$

Fig. 2. Physical diagram of the HC system

where $R(t)$ is the accumulative combustible recovery at flotation time t, R_∞ represents the ultimate recovery, and k is the rate constant.

Xu (1998) corrected based on the first-order model and proposed the calculation of selectivity:

$$K_m = R_\infty \times k = \frac{\partial R}{\partial t}\Big| t=0 \tag{5}$$

$$SI(I/II) = \frac{K_m \ of \ Mineral \ I}{K_m \ of \ Mineral \ II} \tag{6}$$

where K_m is the modified rate constant and SI is the selectivity index. The parameter k is the first-order rate constant. In this study, mineral I and II represent the ash material and the combustible matter.

The selectivity index and flotation rate constant are effectively to evaluate the flotation processes.

3. Results and discussion

3.1. Flotation experiments

Fig. 3 shows the flotation results for the coal sample obtained in *CGB* and ultrapure water. It can be concluded from Fig. 3 that when the flotation time was less than 150 s, the clean coal yield of synthetic *CGB* was higher than that of ultrapure water. However, when the time increases further to 180 s, the value of synthetic *CGB* is slightly smaller than that of ultrapure water. The ash content of clean coal is no big change with the accumulation of time. The ash content of ultrapure water (about 14.5%) is 1.6% greater than that of synthetic *CGB* (about 13.9%) at different times. Table 4 shows the first-order rate constant (k), the modified rate constant (K_m), the ultimate recovery (R_∞), and the selectivity index (SI) values of *CGB* and ultrapure water. The values in Table 4 reveal that the rate constant of synthetic *CGB* solution is more prominent than that of ultrapure water; it means the clean coal can be floated more quickly in a limited time than ultrapure water. The ultimate recovery of synthetic *CGB* is smaller than that of ultrapure water, and it corresponds to the last clean coal yield. The SI value of synthetic *CGB* (7.086) is twice as many as that of ultrapure water (3.545), and it infers that the flotation selectivity of synthetic *CGB* used as a flotation solution is better.

Three synthetic solutions that contain NaCl, $MgCl_2$, and $CaCl_2$ individually were used for the flotation experiments. The comparisons of the clean coal yield and ash content among ultrapure water, NaCl, $MgCl_2$, and $CaCl_2$ solutions are shown in Figs. 4 and 5. In Fig. 4, it can be seen that the coal yield at 180 s decreases from 65.41% to 59.50%, when replacing ultrapure water with single saline water.

Within the different single saline water, the clean coal yield in NaCl solution is lower 8% than $MgCl_2$ and $CaCl_2$ saline solutions in the first 30 s. The clean coal yield of NaCl, $MgCl_2$, and $CaCl_2$ reach at the same level at 120 s.

As shown in Fig. 5, the single saline water ($MgCl_2$ solution) can also decrease by about 2.9% of the ash content in comparison to the usage of ultrapure water. The ash content of NaCl solution is higher than those of $MgCl_2$ and $CaCl_2$ solutions, and it decreases along with the flotation time. To be noted, the ash content of NaCl, $MgCl_2$, and $CaCl_2$ solutions approaches to nearly the same level at 180 s.

Table 4. The *SI* values of synthetic *CGB* and ultrapure water

Solution	Ash			Combustible matter			SI
	K	R_∞	K_m	K	R_∞	K_m	
Ultrapure	0.017	27.129	0.463	0.018	91.750	1.640	3.545
synthetic CGB	0.012	21.596	0.262	0.022	83.076	1.859	7.086
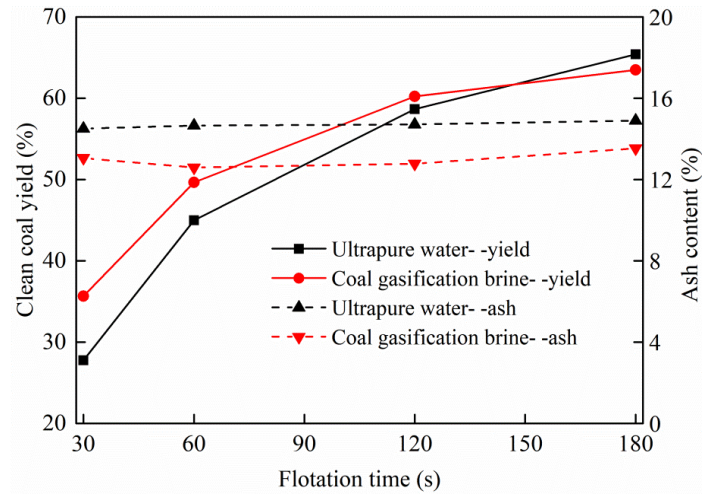
Fig. 3. Flotation results of coal sample in synthetic *CGB* and ultrapure water
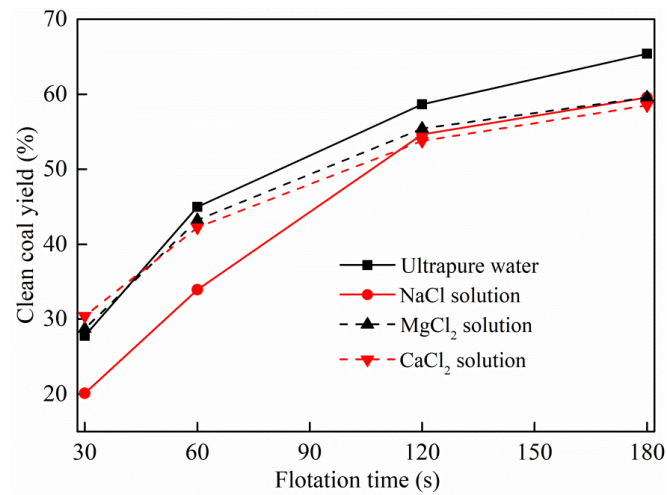
Fig. 4. The clean coal yield of ultrapure water, NaCl, MgCl$_2$, and CaCl$_2$ solutions
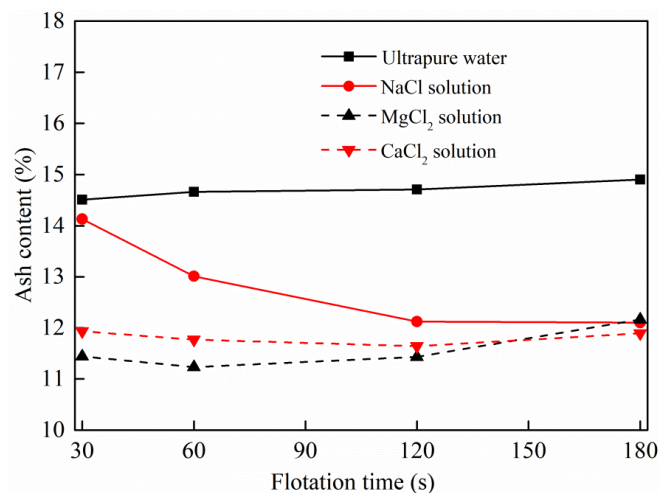
Fig. 5. The ash content of clean coal obtained in ultrapure water, NaCl, MgCl$_2$, and CaCl$_2$ solutions

Table 5 gives the *SI* values of single saline water and ultrapure water. As shown in Table 5, the K_m values of ash and the combustible recovery of NaCl solution are the smallest, while the R_∞-value of the combustible content recovery is the highest. Though the values of first-order rate constant (k) for MgCl$_2$ and CaCl$_2$ solutions are greater than those for NaCl and ultrapure water, the values of the ultimate

recovery of combustible content (R_∞) for $MgCl_2$ and $CaCl_2$ are lower than those for NaCl and ultrapure water, which verifies the variation of coal yield and ash content. The saline solutions were sorted in order of *SI* values size: $MgCl_2$ > $CaCl_2$ > NaCl > ultrapure. It was concluded that Mg^{2+} and Ca^{2+} had superior ability to improve the separation selectivity of coal flotation compared to Na^+.

Table 5. The *SI* values of single saline water and ultrapure water

Solution	Ash content recovery			Combustible content recovery			*SI*
	k	R_∞	K_m	k	R_∞	K_m	
Ultrapure	0.017	27.129	0.463	0.018	91.750	1.640	3.545
NaCl	0.014	21.071	0.305	0.011	97.864	1.119	3.669
$MgCl_2$	0.018	19.722	0.362	0.021	85.049	1.814	5.005
$CaCl_2$	0.023	18.463	0.420	0.023	82.272	1.865	4.437

3.2. Effects of monovalent and divalent ions on froth entrainment

With different configurations of solutions, the ash content distributions of clean coal at the first 30s floatation are shown in Fig. 6. Instead of ultrapure water and NaCl solution, $MgCl_2$ and $CaCl_2$ solution can decrease the ash content of each grade. The results illustrate that the NaCl solution can only reduce the ash content of -0.074 mm particles. The ash content of 0.5-0.25 mm and 0.25-0.074 mm in NaCl solution is both slightly higher than that in ultrapure water.
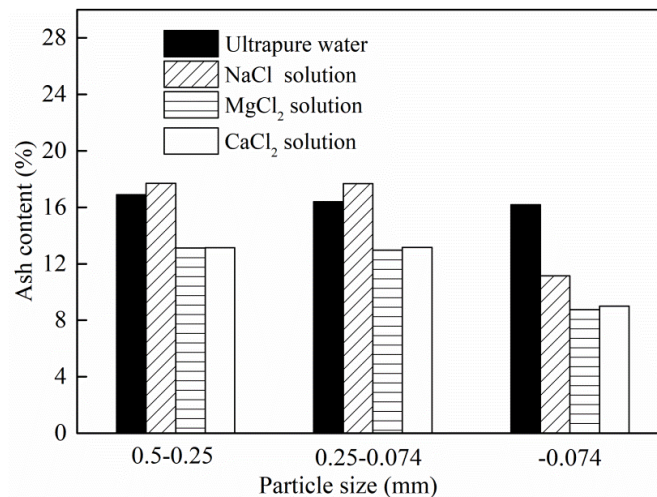
Fig. 6. The ash content distribution of clean coal at the first 30 s floatation

The recovery of fine particles (-0.074 mm) is primarily due to water recovery or entrainment rather than true flotation via bubble attachment, which can be associated with the small mass and high specific surface area (Bu et al., 2017b). It is stated that reducing the water entrainment could lower the ash content of fine coals (Liang et al., 2015). The water entrainment mainly rests on the parameters of air bubbles. Neethling et al.(2003) found that the velocity of the liquid film was inversely proportional to the diameter of the bubble so that the recovery of water and the water entrainment were reduced with the increasing of bubble size. The surfaces of coarse coal particles (0.5-0.074 mm) were compressed by positive ions, and further influence the contact of coals and bubbles (presented in sections 3.3). The recovery processes of coarse and fine particles together determine the ash content and yield of clean coal.

The images in Fig. 7 were captured in 18 s after collecting the concentration. The imagines were analyzed with Image J software. Five largest bubbles in the diameter of each image were selected to measure by the line tool. The average of 5 values was marked as the diameter of bubbles in each saline solution. The values were calculated as 13, 8, 17, 15 mm from image A to D of Fig. 7 respectively. It was obvious that the average size of the bubbles was bigger in $MgCl_2$ and $CaCl_2$ solution than that in NaCl

solution and ultrapure water. The average sizes of the bubble in NaCl solution and ultrapure water have little difference from images, but the diameters of bubbles in NaCl solution were the smallest from the data. Lessard and Zieminski (Lessard and Zieminski, 1971) investigated the effects of various electrolytes on bubble coalescence and interfacial gas transfer in aqueous solution. They defined the transition concentration, at which coalescence was sharply reduced. The transition concentrations for NaCl, MgCl$_2$, and CaCl$_2$ are 0.175, 0.055, and 0.055 mol/dm^3, respectively. In this study, the concentrations of 0.020 MgCl$_2$ and 0.015 mol/dm^3 CaCl$_2$ were lower than their transition concentrations. Those findings are in agreement with the literature (Gungoren et al., 2018). Therefore, the presence of MgCl$_2$ and CaCl$_2$ can promote the bubble coalescence. However, the concentration of NaCl of this work (0.34 mol/dm^3) is greater than its transition concentration, which leads to a reduction of coalescence between bubbles. This agrees with the measurement results of the average bubble size in Fig. 7.

The average water recovery rate in flotation is shown in Fig. 8. The average water recovery rate of the first 30s showed that the ultrapure water entrainment could achieve the maximal. Therefore, NaCl, MgCl$_2$, and CaCl$_2$ solutions can reduce the water entrainment so that the ash content of clean coal was reduced either.
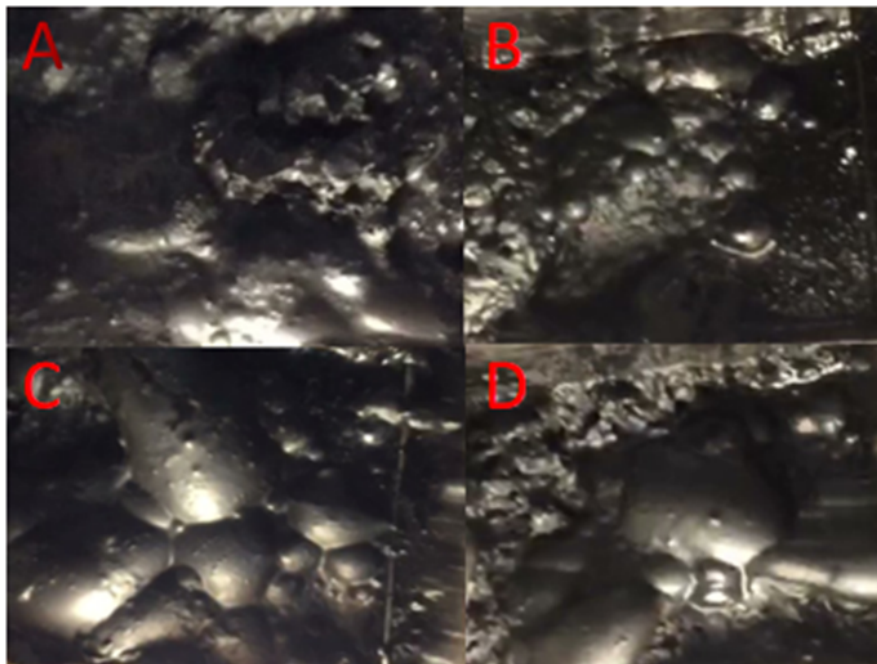
Fig. 7. Images of air bubbles in flotation. A, B, C, and D is the air bubble in the ultrapure water, 0.340 mol/dm^3 NaCl, 0.020 mol/dm^3 MgCl$_2$, and 0.015 mol/dm^3 CaCl$_2$ solution, respectively
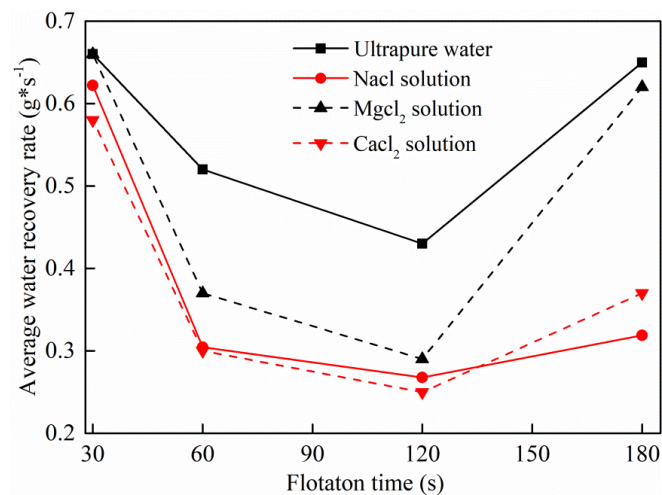
Fig. 8. The average water recovery rate in flotation

3.3. Effects of monovalent and divalent ions on the interaction between coal particles and bubbles

The induction times of four solutions are measured separately, and the results are shown in Fig 9. The induction time of bubbles and coals in NaCl solution was a little shorter than that in ultrapure water. The induction time of $CaCl_2$ solution was less than half of ultrapure water. $MgCl_2$ and $CaCl_2$ saline solutions flotation could reduce the induction time of coal and air bubbles, however, the NaCl solution had an insignificant effect. It is demonstrated that the presence of salt ions facilitates to trigger the film rupture process and shorten the attachment time between coal particles and gas bubbles compared to the ultrapure water. It is well known that the main reason for poor coarse particle recovery is the high probability of detachment between particles and gas bubbles (Tao, 2004). Therefore, a shorter attachment time produced by the *CGB* can diminish the attachment probability between coarse coal particles (>0.074 mm) and gas bubbles compared to that of ultrapure water. The *CGB* promotes the recovery of coarse coal particles having low ash content, which are in good agreement with the reduction of ash content of 0.5-0.074 mm size fractions shown in Fig. 6.

The compression of the electrical double layer in saline water enhances the thinning and rupture of the wetting film between bubbles and particles, which are a critical step in the formation of a stable bubble-particle aggregate.
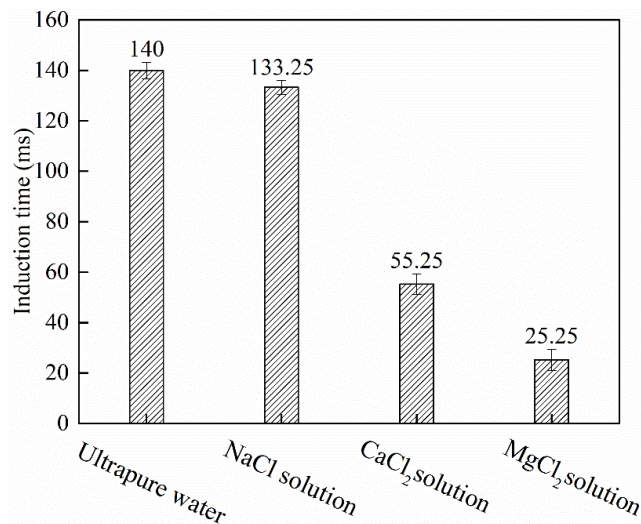
Fig. 9. Induction time of coal particles in the four solutions

The zeta potentials of coal and bubbles in single saline solutions and ultrapure water are shown in Fig. 10. Based on the observations of the literature (Hasegawa et al., 2008; Takahashi, 2005), there is no relationship between the zeta potential of air bubbles and the bubble size, i.e., the zeta potential of bubbles is independent of the bubbles diameter. Therefore, the measured zeta potential of nanobubbles generated using hydrodynamic cavitation was approximately used as the zeta potential of flotation bubbles. The coal particles and the gas bubbles are negatively charged, resulting in a repulsive double-layer force between the bubble and the coal particle. It can be seen from Fig. 10 that whether the absolute values of coal or bubbles in ultrapure water were the maximal compared to the other three saline solutions. NaCl solution could reduce the limited absolute values of zeta potential but the influences of $MgCl_2$ and $CaCl_2$ solutions were significant. Therefore, $MgCl_2$ and $CaCl_2$ saline solutions can compress the electric double layer and reduce the zeta potential. The control of the zeta potentials of bubbles and silica surfaces to create attractive electrical double-layer (*EDL*) forces could improve the kinetics of film thinning, which is conducive to promoting bubble-particle attachment in flotation (Huang K, 2020). Thus, Mg^{2+} and Ca^{2+} promoted the attachment between coal particles and bubbles, which is in good agreement with the experimental results of induction time and flotation performance.

To explain the experimental results of induction time theoretically, the interaction between coal and bubbles were calculated according to the DLVO theory. The van der Waals energy (E_V) (Zhou et al., 2020) and double electric layer interaction energy (E_E) (Yoon, 2000) were calculated using Eq. 7:
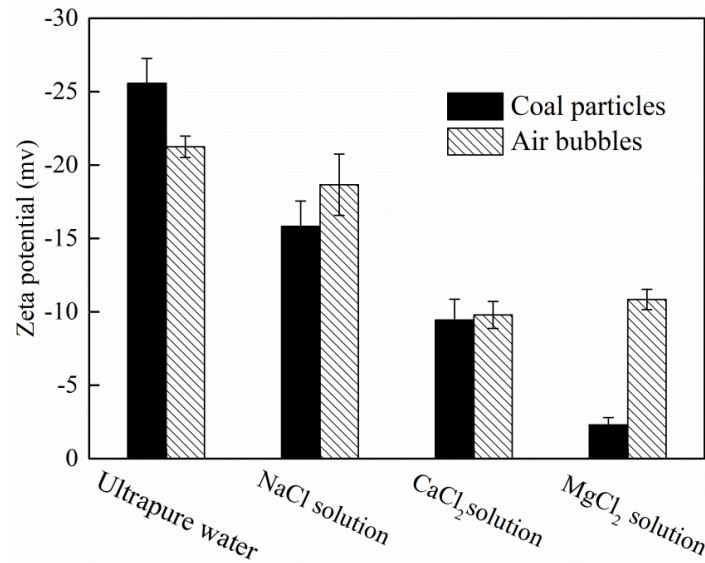
Fig. 10. The zeta potentials of coal particles and air bubbles in four solutions

$$E_V = -\frac{A_{132}R_1R_2}{6H(R_1+R_2)} \tag{7}$$

where R_1 and R_2 are the radii of the two spheres (the radius of nano-bubble is 3.94 nm in this experience). H is the value of the distance between the spheres. A_{132} is Hamaker constant with value of 4.84×10^{-20} J.

$$E_E = \frac{\pi\varepsilon_0\varepsilon R_1R_2}{R_1+R_2}\left(\varphi_1^2+\varphi_2^2\right)\left[\frac{2\varphi_1\varphi_2}{\varphi_1^2+\varphi_2^2}\, p + q\right] \tag{8}$$

$$p = \ln\left[\frac{1+\exp\,(-\kappa H)}{1-\exp\,(-\kappa H)}\right] \tag{9}$$

$$q = \ln[1 - \exp(-\kappa H)] \tag{10}$$

$$\kappa^{-1} = [\varepsilon\varepsilon_0 k_B T \textstyle\sum_i n_i Z_i^2 e^2]^{1/2} \tag{11}$$

where φ_1 and φ_2 represent the surface potentials of spheres 1 and 2 respectively, ε_0 and ε are the values of absolute permittivity in the dispersion medium (78.5F/m) and vacuum ($8.84 \times 10\text{-}12$ F/m)(Zhou et al., 2020), respectively, κ^{-1} is the Debye length (the double-layer thickness) and the equation of different solutions is written in Eq. (11) (Ishikawa et al., 2005). Where e is the elementary electric charge, n_i is the number of ions of type i per unit volume in the bulk solution, Z_i is the valency of ion i, k_B is the Boltzmann constant, and T is the absolute temperature. For 0.001 mol/dm³ NaCl solution at 25℃ the double-layer thickness is approximately 9.6 nm (Gupta et al., 2011). In the case of NaCl, MgCl₂, and CaCl₂ solutions, similar curves for the dependence of the double-layer interaction energy on the separation and the electrolyte concentration are obtained using the available zeta potentials. The concentration of ions of type i in the bulk solution is given by:

$$n_i = 1000 \times C_i \tag{12}$$

The main parameters used in κ^{-1} calculation were given in Table 6. The calculation results of κ^{-1} in different solutions are given in Table 7.

Table 6. Parameters used in κ^{-1} calculation

Elementary charge (e) / C	Relative permittivity of water (ε_r)	Permittivity of a vacuum (ε_0) / C² J⁻¹ m⁻¹	Boltzmann constant (k_B) / J·K⁻¹	Avogadro constant (N_A) / mol⁻¹
1.602×10^{-19}	78.5	8.854×10^{-12}	1.38×10^{-23}	$6.023\times10^{+23}$

Table 7. Calculation results of κ^{-1} in different solutions.

solutions	NaCl	CaCl₂	MgCl₂	Ultrapure water
κ^{-1}/m	5.20×10^{-10}	1.40×10^{-09}	1.30×10^{-09}	9.6×10^{-09} [a]

[a] the κ^{-1} values for 0.001 mol/dm³ NaCl solution were approximately used as the κ^{-1} of ultrapure water in simplification

It depends on the size of the energy barrier (E_T) that whether the coal particles can adhere to the bubbles or not. However, the energy barrier is the sum of van der Waals energy (E_v) and double electric layer interaction energy (E_E) (Guo et al., 1999). The energy barrier was calculated further, and the results were shown in Fig. 11. The value of the energy barrier between coal particles and bubbles in ultrapure water is always higher than that in the other three solutions. It means that Na^+, Mg^{2+}, and Ca^{2+} can reduce the double electric layer interaction energy (E_E) and it is obvious that divalent ions of Ca^{2+} and Mg^{2+} have a more significant influence on the on the size of E_T than that of Na^+. Compared to ultrapure water, the repulsive double-layer force between coal particles and gas bubbles can be minimized when *CGB* was employed due to compression of the double layer and the resulting reduction of the zeta potential. The compression of the electrical double layer in saline water enhances the thinning and rupture of the wetting film between bubbles and particles, which are a critical step in the formation of a stable bubble-particle aggregate (Zhang et al., 2019). Thus, the calculated results of the DLVO theory are consistent with the results of induction time.
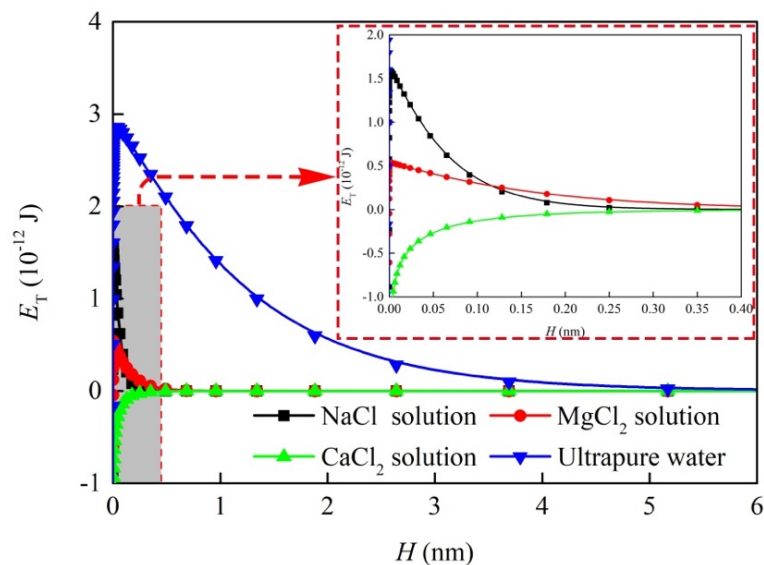
Fig. 11. The interaction energy between coal particle and gas bubble in different solutions

4. Conclusions

The effect of monovalent and divalent ions (Na^+, Mg^{2+}, and Ca^{2+}) in coal gasification brine on the froth entrainment and flotation kinetics of anthracite coal could be summarized as follows:

- The SI value of synthetic *CGB* (7.086) is twice as many as that of ultrapure water (3.545), it shows that the flotation selectivity of synthetic *CGB* is better to ultrapure water. Mg^{2+}, and Ca^{2+} affords superior performance over Na+ by enhancing the separation selectivity of coal flotation.
- The primary positive ions Na^+, Mg^{2+}, and Ca^{2+} in *CGB* were manual configurations, and each of the ions can reduce the ash content of coal size below 0.074 mm because the ions reduce the entrainment of water effectively by influence the air bubbles.
- $MgCl_2$ and $CaCl_2$ solutions can also reduce the ash content of coarse coal particles (> 0.074 mm) and promote the interaction between coal particles and bubbles by the reduction of the energy barrier between coal particles and gas bubbles.
- The synthetic *CGB* has good prospects for the development and application in coal flotation, which opens up a new way for recycling.

References

ARNOLD, B.J., APLAN, F.F., 1986. *The effect of clay slimes on coal flotation, part II: The role of water quality*. Int. J. Miner. Process. 17, 243-260.

BOURNIVAL, G., MUIN, S.R., LAMBERT, N., ATA, S., 2017. *Characterisation of frother properties in coal preparation process water*. Miner. Eng. 110, 47–56.

BOURNIVAL, G., ZHANG, F., ATA, S., 2019. *Coal Flotation in Saline Water: Effects of Electrolytes on Interfaces and Industrial Practice*. Miner. Process. Extr. Metall. Rev. 0, 1–21.

BU, X., CHEN, Y., MA, G., SUN, Y., NI, C., XIE, G., 2019. *Differences in dry and wet grinding with a high solid concentration of coking coal using a laboratory conical ball mill : Breakage rate , morphological characterization , and induction time*. Adv. Powder Technol. 30, 2703–2711.

BU, X., XIE, G., CHEN, Y., NI, C., 2017a. *The Order of Kinetic Models in Coal Fines Flotation*. Int. J. Coal Prep. Util. 37, 113–123.

BU, X., XIE, G., PENG, Y., 2017b. I*nteraction of fine, medium, and coarse particles in coal fines flotation*. Energy Sources, Part A Recover. Util. Environ. Eff. 39, 1276–1282.

BU, X., XIE, G., PENG, Y., GE, L., NI, C., 2017c. *Kinetics of flotation. Order of process, rate constant distribution and ultimate recovery*. Physicochem. Probl. Miner. Process. 53, 342–365.

BU, X., ZHANG, T., CHEN, Y., PENG, Y., XIE, G., WU, E., 2018. *Comparison of mechanical flotation cell and cyclonic microbubble flotation column in terms of separation performance for fine graphite*. Physicochem. Probl. Miner. Process. 54, 732–740.

ERSOY, Ö., TURGUT, H., GUVEN, O., ÇINKU, K., OZDEMIR, O., CELIK, M., 2013. *Effect of heat treatment on the flotation of Turkish lignites in brine solution*, in: Materials Science and Technology Conference and Exhibition 2013, MS and T 2013.

FANG, F., HAN, H., 2018. Effect of Catalytic Ozonation Coupling with Activated Carbon Adsorption on Organic Compounds Removal Treating RO Concentrate from Coal Gasification Wastewater. Ozone Sci. Eng. 40, 275–283.

FUERSTENAU, D.W., ROSENBAUM, J.M., LASKOWSKI, J., 1983. E*ffect of surface functional groups on the flotation of coal*. Colloids and Surfaces 8, 153–173.

GAMAL, R., EDRESS, N.A.A., EL-MIDANY, A.A., EL-MOFTY, S.E., 2018. *Valuation of chloride salts and their mixtures in coal flotation without collector*. Energy Sources, Part A Recover. Util. Environ. Eff. 40, 2822–2831.

GUNGOREN, C., ISLEK, E., BAKTARHAN, Y., UNVER, I.K., OZDEMIR, O., 2018. *A novel technique to investigate the bubble coalescence in the presence of surfactant (MIBC) and electrolytes (NaCl and CaCl₂)*. Physicochem. Probl. Miner. Process. 54, 1215–1222.

GUO, L.X., OU, Z.S., HU, M.X., 1999. E-*DLVO theory and its application in coal slurry suspension*. Chinese Min. Mag. 8, 69–72.

GUPTA, V., HAMPTON, M.A., STOKES, J.R., NGUYEN, A. V., MILLER, J.D., 2011. *Particle interactions in kaolinite suspensions and corresponding aggregate structures*. J. Colloid Interface Sci. 359, 95–103.

GUPTA, V.K., ALI, I., SALEH, T.A., NAYAK, A., AGARWAL, S., 2012. *Chemical treatment technologies for waste-water recycling - An overview*. RSC Adv. 2, 6380–6388.

HARVEY, P.A., NGUYEN, A. V., EVANS, G.M., 2002. *Influence of electrical double-layer interaction on coal flotation*. J. Colloid Interface Sci., 250, 337-343.

HASEGAWA, H., NAGASAKA, Y., KATAOKA, H., 2008. *Electrical potential of microbubble generated by shear flow in pipe with slits*. Fluid Dyn. Res. 40, 554–564.

HUANG K, Y.R.H., 2020. *Control of bubble ζ-potentials to improve the kinetics of bubble-particle interactions*. Miner. Eng., 151, 106295

ISHIKAWA, Y., KATOH, Y., OHSHIMA, H., 2005. *Colloidal stability of aqueous polymeric dispersions: Effect of pH and salt concentration*. Colloids Surfaces B Biointerfaces 42, 53–58.

JIA, S., HAN, H., ZHUANG, H., XU, P., HOU, B., 2015. *Advanced treatment of biologically pretreated coal gasification wastewater by a novel integration of catalytic ultrasound oxidation and membrane bioreactor*. Bioresour. Technol. 189, 426–429.

JIA, S., ZHUANG, H., HAN, H., WANG, F., 2016. *Application of industrial ecology in water utilization of coal chemical industry: A case study in Erdos, China*. J. Clean. Prod. 135, 20–29.

KLASSEN, V., MOKROUSOV, V., 1963. *An Introduct4ion to the Theory of Flotation*. Chem. Eng. News, LONDON.

KURNIAWAN, A.U., OZDEMIR, O., NGUYEN, A. V., OFORI, P., FIRTH, B., 2011. *Flotation of coal particles in MgCl2, NaCl, and NaClO 3 solutions in the absence and presence of Dowfroth 250*. Int. J. Miner. Process. 98, 137–144.

LASKOWSKI, J., ISKRA.J, 1970. *Role of Capillary Effects in Bubble-Particle Collision in Flotation*. Trans. Inst. Min. Met C1–C6.

LESSARD, R.R., ZIEMINSKI, S.A., 1971. *Bubble Coalescence and Gas Transfer in Aqueous Electrolytic Solutions*. Ind. Eng. Chem. Fundam. 10, 260–269.

LI, C., SOMASUNDARAN, P., 1993. *Role of Electrical Double Layer Forces and Hydrophobicity in Coal Flotation in NaCl Solutions*. Energy and Fuels, 7, 244-248..

LI, G., DENG, L., CAO, Y., WANG, B., RAN, J., ZHANG, H., 2017. *Effect of sodium chloride on fine coal flotation and discussion based on froth stability and particle coagulation*. Int. J. Miner. Process. 169, 47–52.

LI, K., MA, W., HAN, H., XU, C., HAN, Y., WANG, D., MA, WEIWEI, ZHU, H., 2018. *Selective recovery of salt from coal gasification brine by nanofiltration membranes*. J. Environ. Manage. 223, 306–313.

LIANG, L., LI, Z., PENG, Y., TAN, J., XIE, G., 2015. *Influence of coal particles on froth stability and flotation performance*. Miner. Eng. 81, 96–102.

NEETHLING, S.J., LEE, H.T., CILLIERS, J.J., 2003. *Simple relationships for predicting the recovery of liquid from flowing foams and froths*. Miner. Eng. 16, 1123–1130.

OZDEMIR, O., 2013. *Specific ion effect of chloride salts on collectorless flotation of coal*. Physicochem. Probl. Miner. Process. 49, 511–524.

OZDEMIR, O., ERSOY, O.F., GUVEN, O., TURGUT, H., CINAR, M., ÇELIK, M.S., 2018. I*mproved flotation of heat treated lignite with saline solutions containing mono and multivalent ions*. Physicochem. Probl. Miner. Process. 54, 1070–1082.

OZDEMIR, O., TARAN, E., HAMPTON, M.A., KARAKASHEV, S.I., NQUYEN, A. V., 2009. *Surface chemistry aspects of coal flotation in bore water*. Int. J. Miner. Process. 92, 177–183.

PUGH, R.J., WEISSENBORN, P., PAULSON, O., 1997. *Flotation in inorganic electrolytes; The relationship between recover of hydrophobic particles, surface tension, bubble coalescence and gas solubility*. Int. J. Miner. Process. 51, 125-138

TAKAHASHI, M., 2005. *ζ Potential of Microbubbles in Aqueous Solutions: Electrical Properties of the Gas−Water Interface*. J. Phys. Chem. B 109, 21858–21864.

TAO, D., 2004. *Role of Bubble Size in Flotation of Coarse and Fine Particles - A Review*. Sep. Sci. Technol. 39, 741–760.

VERRELLI, D.I., ALBIJANIC, B., 2015. *A comparison of methods for measuring the induction time for bubble-particle attachment*. Miner. Eng. 80, 8–13.

WANG, B., PENG, Y., 2014. *The effect of saline water on mineral flotation - A critical review*. Miner. Eng. 66, 13–24.

WANG, B., PENG, Y., VINK, S., 2014. E*ffect of saline water on the flotation of fine and coarse coal particles in the presence of clay minerals*. Miner. Eng. 66, 145–151.

WANG, H., ZHU, H., ZHU, J., TANG, J., HUANG, D., SHAO, S., 2019. *Optimizing oxidized coal flotation through pH adjustment and inorganic salt ion*. Int. J. Coal Prep. Util. 0, 1–9.

WEI, T., PENG, Y., VINK, S., 2016. *The joint action of saline water and flotation reagents in stabilizing froth in coal flotation*. Int. J. Miner. Process. 148, 15–22.

XIONG, L., YU, G., SUN, Y., 2015. *Application of strong brine from coal chemical industry in coal slime water settling*. Water Wastewater Eng. 21, 5–8.

XU, M., 1998. *Modified flotation rate constant and selectivity index*. Miner. Eng. 11, 271–278.

XU, Z., YOON, R.H., 1990. *A study of hydrophobic coagulation*. J. Colloid Interface Sci. 134, 427-434.

YANG, G.C.C., MARKUSZEWSKI, R., WHEELOCK, T.D., 1988. *Oil agglomeration of coal in inorganic salt solutions*. Coal Prep. 5, 133–146.

YE, Y., MILLER, J.D., 1988. Bubble/particle contact time in the analysis of coal flotation. Coal Prep. 5, 147–166.

YOON, R.-H., SABEY, J.B., 1983. *Coal flotation in Inorganic salt solutions*, in: Botsaris, G.D., Glazman, Y.M. (Eds.), Interfacial Phenomena in Coal Technology. Marcel Dekker, Inc., New York and Basel, pp. 87–114.

YOON, R.-H., YORDAN, J.L., 1991. I*nduction time measurements for the quartz−amine flotation system*. J. Colloid Interface Sci. 141, 374–383.

YOON, R., 2000. *The role of hydrodynamic and surface forces in bubble-particle interaction*. Int. J. Miner. Process. 58, 129–143.

YOON, R.H., 1982. *Flotation of Coal Using Micro-bubbles and Inorganic Salts*. Min. Congr. J. 68, web.

ZHANG, N., CHEN, X., NICHOLSON, T., PENG, Y., 2019. *The effect of saline water on the settling of coal slurry and coal froth*. Powder Technol. 344, 161–168.

ZHOU, S., WANG, X., BU, X., WANG, M., AN, B., SHAO, H., NI, C., PENG, Y., ZIE, G., 2020. *A novel flotation technique combining carrier flotation and cavitation bubbles to enhance separation efficiency of ultra-fine particles.* Ultrason. Sonochem. 64, 105005.